WAVELET BASED SMOKE DETECTION METHOD WITH RGB CONTRAST-IMAGE AND SHAPE CONSTRAIN

Jiaqiu Chen[a], *Yaowei Wang*[a*], *Yonghong Tian*[b], *Tiejun Huang*[b]

[a]School of Information and Electronics, Beijing Institute of Technology, Beijing 100081, China
[b]Institue of Digital Media, Peking University, Beijing, 100871, P.R. China
[*]Corresponding to: yaoweiwang@gmail.com; ywwang@jdl.ac.cn

ABSTRACT

Smoke detection in video surveillance is very important for early fire detection. A general viewpoint assumes that smoke is a low frequency signal which may smoothen the background. However, some pure-color objects also have this characteristic, and smoke also produces high frequency signal because the rich edge information of its contour. In order to solve these problems, an improved smoke detection method with RGB Contrast-image and shape constrain is proposed. In this method, wavelet transformation is implemented based on the RGB Contrast-image to distinguish smoke from other low frequency signals, and the existence of smoke is determined by analyzing the combination of the shape and the energy change of the region. Experimental results show our method outperforms the conventional methods remarkably.

Index Terms— Smoke detection, wavelet transform, RGB Contrast-image, shape constrain

1. INTRODUCTION

Smoke detection plays a vital role in early fire detection, because in many situations smoke appears at the early stage of fire. Based on many characteristics of smoke, such as color[1], motion[2], texture[3], and so on, a lot of methods for smoke detection have been proposed. Among all of these methods, wavelet based methods occupy an important place. They can be roughly divided into two categories: (i) wavelet is used to obtain decomposed images through various subbands, so that smoke's features can be extracted at different resolutions and frequencies. (ii) Wavelet is used to obtain the energy features of both the current frame and the background which will be used in the following analyses. In this paper, the second type of approaches are referred as the conventional wavelet based methods.

Compared with the first category, the conventional wavelet based methods are more generally adopted. In Toreyin et al.[4], wavelet transformation was performed on both the background and the current frame, and the region of the decreased high frequency energy component was identified as smoke, and further he improved his method using Hidden Markov Model(HMM) to mimic the temporal behavior of the smoke on the basis of the periodic behavior of smoke boundaries[5]. Wei et al.[6] used a fuzzy rate V to reflect the characteristics of smoke-obscured edge regions. The rate was the ratio of the decrease in energy and time. Calderara et al.[7] calculated the energy rate of the background and the current frame of every block to support the analysis. Almost all of these methods suppose that the smoke blurs the background, and leads to the loss of the high frequency energy of the background; however, these methods may not work in the following situations: (i) some pure-color objects appear in the scene may also lead to the loss of high frequency energy of the background; (ii) certain background has a small amount of high frequency energy; therefore, no high frequency energy will lose, even if smoke appears; (iii) the non-uniform smoke appeared in the background contains rich edges information. Fig. 1 is an example that illustrates the situations above. The above images are original images and the below are energy images (We obtained the images by using wavelet transformation, and the big pixel value corresponds to high frequency.), it can be seen that the areas where smoke appeared don't lose high frequency, in contrast, high frequency energy is increased. There are two reasons which may lead to the result, for one thing the background shows the characteristic of low frequency, for another smoke's edges contains rich high frequency energy information. In order to overcome the limita-

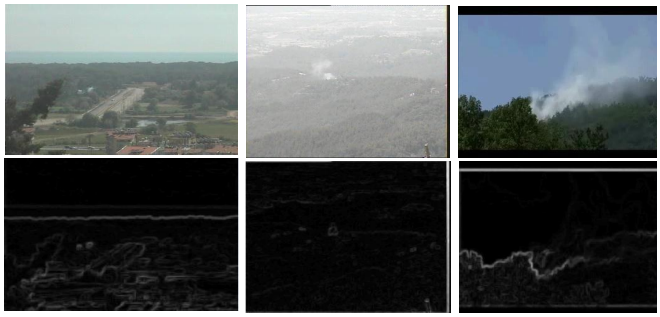

(a) (b) (c)

Fig. 1. The energy images of conventional wavelet.

tions of the conventional wavelet based methods, an improved smoke detection method is introduced with RGB Contrast-image and shape constrain. RGB Contrast-image is the gray level image of original image, which can presents the contrast of R, G, B three channels. In this method, wavelet transformation is implemented based on the RGB Contrast-image to distinguish smoke from other pure-color objects; then the energy change (between background and current frame) of the candidate smoke region which obtained from wavelet transformation is considered together with the shape of the region to support the analysis.

The contributions of this paper are summarized as follow:

(1) The concept of RGB Contrast-image has been introduced, using which the smoke can be distinguished from pure-color objects easily;

(2) RGB Contrast-image is also applied to solve the problems that smoke can not be recognized caused by the totally low frequency characteristic of background (such as pure-color).

(3) Both the loss of high frequency energy in the smoke region and the high frequency energy produced by the edge of the smoke are combined with the shape of the smoke to support the analysis

The rest of this paper is organized as follow: Section 2 explains the general smoke detection processes with the emphasis on the improvement of the purposed method. The detailed results are presented in Section 3. Finally, Section 4 gives the conclusion of the paper.

2. OUR FRAMEWORK

The proposed method can be divided into the following procedures: (i) a background estimation method is used to determine the candidate smoke regions; (ii) a wavelet based smoke detection method with RGB Contrast-image and shape constrain is used to detect the energy characteristic of the candidate smoke regions; (iii) color and motion features are utilized to test the color and motion characteristics of candidate smoke regions. The regions that meet all the criteria of energy, color and motion are identified as smoke.

2.1. Detect candidate smoke regions

The candidate smoke regions in the video are determined by using a background estimation method developed by Collins et al.[8]. First of all, the difference value of current frame and background is obtained with Eq. (1)

$$DI_n(i,j) = |I_n(i,j) - B_n(i,j)| \tag{1}$$

Where B_n denotes current background, I_n denotes current frame, and $DI_n(i,j)$ stores the every pixel's absolute difference of them. Then, Eq. (2) is used to obtain foreground image,

$$FI_n(i,j) = \begin{cases} 1, & DI_n(i,j) > Th_b \\ 0, & DI_n(i,j) \leq Th_b \end{cases} \tag{2}$$

where FI_n denotes the foreground image, Th_b is a threshold which used to turn current frame into a binary image, the Th_b rangs from 20 to 30, in our experiment we set it to 25. When a pixel's value is set to 1, it means this pixel belong to foreground pixel and all the foregrounds pixel form the candidate smoke regions. The value 0 represents the background. The candidate smoke regions is needed to check their energy characteristic and vision features. Finally, when $FI_n(i,j) = 1$ (which means (i,j) is a foreground pixel) we use Eq. (3) to update the background.

$$B_{n+1}(i,j) = \alpha B_n(i,j) + (1-\alpha) I_n(i,j) \tag{3}$$

Where α controls the speed of current frame blends into the background, smaller α corresponds to faster update speed of background, the α rangs from 0.75 to 0.98, we set it to 0.94 in our experiment.

2.2. Wavelet based smoke detection with RGB Contrast-image and shape constrain

2.2.1. Obtain RGB Contrast-image

In this part, the reasons why RGB Contrast-image can differentiate smoke from other low frequency signals are explained and the construction of RGB Contrast-image is introduced.

High frequency usually indicates the edges of an image which implies the values of neighboring pixels have a considerable difference; in contrast, low frequency indicates neighboring pixels have a similar value. Both the appearance of smoke and pure-color objects in the scene could cause the loss of high frequency energy of the background which can lead to false detections. However, since most of smoke is gray, it means the three components of R, G and B have a similar value, whereas general pure-color objects do not have this characteristic. In order to utilize this feature, the values of the three channels are considered separately, and different channels' values are used in the different locations. According to the analyses above, the concept of RGB Contrast-image is introduced, which is the gray level image of original image and it presents three channels' contrast in a neighboring area. The RGB Contrast-image can be obtained by using Eq. (4)

$$CI(i,j) = \begin{cases} Max(R,G,B) & (i+j) mod\, 3 = 0 \\ Median(R,G,B) & (i+j) mod\, 3 = 1 \\ Min(R,G,B) & (i+j) mod\, 3 = 2 \end{cases} \tag{4}$$

Where $CI(i,j)$ denotes the pixel value of RGB Contrast-image in the location (i,j), mod is a function that returns the remainder. R, G, B represent the three channel values of $I_n(i,j)$, the values of Max, $Median$, Min denote the max

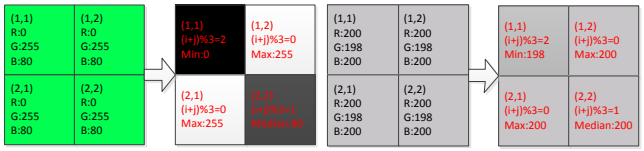

(a) Green(other pure-color objects) (b) Gray(smoke)

Fig. 2. Compare smoke with other pure-color objects.

value, median value and min value of R, G and B. Fig. 2 is used as a sample to explain the Eq. (4). Fig. 2(a) stands for the pure-color objects and Fig. 2(b) stands for the smoke. It can be seen, both the left sub-images (original image) of Fig. 2(a) and Fig. 2(b) have the characteristic of low frequency; however, the right sub-image (RGB Contrast-image) of Fig. 2(a) presents high frequency and Fig. 2(b)'s RGB Contrast-image shows low frequency. If wavelet transformation is performed on both of them, the results may be different.

Through the above analyses, it can be seen that pretreatment on wavelet transformation with RGB Contrast-image is effective to reduce false detection in situations where the background has less edge information or other pure-color objects cover the background.

2.2.2. *Wavelet based method with shape constrain*

In this part, the shape of the candidate smoke region is used to constrain its energy change. After the RGB Contrast-images CI_{I_n} and CI_{B_n} are gotten (by using Eq. (4)), which denote the RGB Contrast-images of the current frame and the background respectively, wavelet transformation is used to obtain an approximation image and three detail images of the RGB Contrast-image which are noted as LL, LH, HL and HH. The energy images of CI_{I_n} and CI_{B_n} are denoted as $E_B(i,j)$ and $E_I(i,j)$ respectively, and they can be calculated by using Eq. (5).

$$E(i,j) = LH(i,j)^2 + HL(i,j)^2 + HH(i,j)^2 \quad (5)$$

Then the energy image is divided into fixed block size of $l \times l$, and every block's energy is calculated by using equation (6).

$$En_k = \sum_{(i,j) \in Block_k} E(i,j) \quad (6)$$

Where En_k describes the energy value of $Block_k$. Conventional wavelet based methods always suppose that if $En_{k,I}$(k th block in the I) has a smaller value then $En_{k,B}$(k th block in the B), the $Block_k$ is a smoke block. Fig. 3 explains the unreasonable of conventional wavelet based methods. Fig. 3(a) is the original image, the above represents smoke which has a big area and a short perimeter, the below means smoke which has a small area and a long perimeter. Use Eq. (4) and Eq. (5) the RGB Contrast-images and energy images can be obtained and showed in Fig. 3(b) and Fig. 3(c). Considering Fig. 3(c), in the above image, smoke region shows low frequency which is conformity with general idea; however, in the below image, the appearance of smoke corresponds to high frequency. It happens because the small area and long perimeter lead to rich edge information in the smoke region.

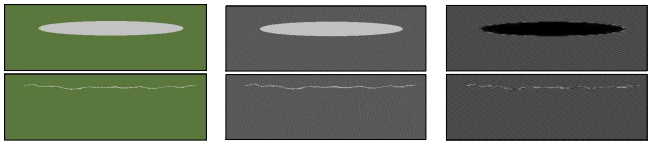

(a) Original image (b) Contrast-image (c) Energy image

Fig. 3. The rate of high frequency and low frequency with different areas and perimeters.

From the example, it can be seen that the shape of the smoke region has a huge effect on the energy change between background and current frame. The variables $Rate_{en}$ and $Rate_{sh}$ are used to describe the rate of $\frac{highfrequency}{lowfrequency}$ and $\frac{perimete}{area}$ respectively, and larger $Rate_{sh}$ corresponds to larger $Rate_{en}$. According to the above analyses, Eq. (7) is used to obtain $Rate_{en}$ and Eq. (8) is used to constrain the relationship of the shape and the energy change of the region.

$$Rate_{en} = (\sum_{k=0}^{N} HE_k)/(\sum_{k=0}^{N} LE_k) \quad (7)$$

In Eq. (7), N is the total number of blocks in the region. HE_k and LE_k are the values of high frequency energy and low frequency energy respectively, and they can be obtained with following steps: get the values of $En_{k,I}$ and $En_{k,B}$ through Eq. (6); (ii) if $En_{k,I} - En_{k,B} > Th_1$, we set $HE_k = 1, LE_k = 0$; else $HE_k = 0, LE_k = 1$. Where Th_1 is a predetermined threshold which limits the range of energy's change and we set it to 0 in our experiment.

$$Rate_{sh} < Th_2 \times Rate_{en} \quad (8)$$

Eq. (8) represents $Rate_{en}$ and $Rate_{sh}$ should meet a proportional relationship, th_2 is the scaling factor,it rangs 0.1 to 1, we set it to 0.6. When Eq. (8) is false, the moving region is identified as non-smoke region, else the region need to be detected its color and motion features.

2.3. Other features

2.3.1. *Color feature*

A video sequence can be expressed as a conjugate of information flows from multiple visual feature channels. The red-green(RG) and blue-yellow(BY) contrast which proposed by Walther et al.[9] are used in our framework, Eq. (9) described how we can get them.

$$RG_k = \frac{r_k - g_k}{max(r_k, g_k, b_k)}, \quad BY_k = \frac{b_k - min(r_k, g_k)}{max(r_k, g_k, b_k)} \quad (9)$$

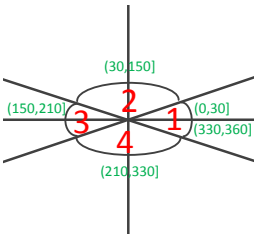

Fig. 4. Opticalflow's direction

Fig. 5. Original image

where RG_k and BY_k are the red-green contrast and blue-yellow contrast respectively. Smoke is always grayish, so the values of RG and BY should be close to zero. In this paper, if most of the blocks in a candidate smoke region satisfy this condition, then the region is temporary seen as smoke region and we need check its motion feature.

2.3.2. Motion feature

The block-based optical flow (proposed by Beauchemin.[10] in 1995) is used to obtain the motion direction and strength of the candidate smoke regions. Suppose I_{velx} and I_{vely} are the images which store the motion information of x direction and y direction respectively. We use Eq. (10) to calculate a pixel's motion direction θ and speed value γ.

$$\begin{aligned} \theta(i,j) &= \tan^{-1}(\tfrac{I_{velx}(i,j)}{I_{vely}(i,j)}) \\ \gamma(i,j) &= \sqrt{I_{velx}(i,j)^2 + I_{vely}(i,j)^2} \end{aligned} \tag{10}$$

Then we code the value of θ into four values, Fig. 4 illustrates the specific method:

(i). $\theta \in (330^o, 360^o] or (0, 30^o], \theta = 1$;
(ii). $\theta \in (30^o, 150^o], \theta = 2$;
(iii). $\theta \in (150^o, 210^o], \theta = 3$;
(iv). $\theta \in (210^o, 330^o], \theta = 4$.

When consider a candidate smoke region we calculate all the blocks' values of θ and if the values of θ are a mixture of all the four values or $\theta = 2$ takes up most of the values, then we believe that the region meet the rule of smoke's motion direction. γ is used to limit smoke's moving speed, we calculate all the blocks' γ in the candidate smoke region and if the average value of all the γs is less than a threshold, then we think the region meet the requirement of smoke's motion speed (In this paper, we suppose the wind in the scene is not big enough to totally affect smoke's moving direction and speed).

3. EXPERIMENTS

The experiment settings are Vs2008 and opencv 2.4.2. The experiments are conducted on eight clips, which from Toreyin et al's[4] open database (http://signal.ee.bilkent. edu.tr/VisiFire/) and B.C. Ko's.[11] database (http://cvpr. kmu.ac. kr).

One of them is chosen as an example to do the following analyses. Fig. 5 is the original smoke image. Fig. 6(a) to Fig. 6(e) and Fig. 6(f) to Fig. 6(j) show the results of Toreyin's method and the proposed method, respectively.

By comparing area A in Fig. 6(c) and area $A1$ in Fig. 6(h), it can be seen that using Toreyin's [4] method the red bin is recognized as low frequency, even if smoke appears, it cannot be detected due to the fact that there is no loss of high frequency energy. On the contrary, in the proposed method, the red bin is detected as high frequency, and when the smoke appears, the high frequency energy will lose.

By comparing area B in Fig. 6(d) and area $B1$ in Fig. 6(i), it can be seen that using Toreyin's [4] method, there is no loss of high frequency energy in the smoke region; on the contrary, high frequency appears. However, in the proposed method, the area $B1$ is presented as low frequency. It is due to the fact that in Toreyin's method, the red bin belongs to low frequency domain at the beginning, and high frequency produced by smoke's contour.

By comparing area $B1$ in Fig. 6(i) and area $C1$ in Fig. 6(i), it can be seen that although there is smoke in both $B1$ and $C1$, $B1$ presents low frequency and $C1$ shows high frequency. It is due to the fact that in area $C1$, the edges occupy most of the smoke region; however, when the smoke area is large enough as area $B1$, the area inside the smoke which corresponds to low frequency overwhelms in the circle.

Fig. 6(e) and Fig. 6(j) show the final results of two methods. The proposed method is more effective compared to Toreyin's method.

The global evaluation measurements proposed by Jakovcevic et al.[12] are also used to evaluate the proposed method. The measurements include true positive rate (TPR),True negative rate (TNR), False negative rate (FNR or missed detection) and false positive rate (FPR). Because $TNR = 100 - FPR$ and $FNR = 100 - TPR$, in this paper we just use TPR and FPR to evaluate our method. Eq. (11) shows how we can get them.

$$TPR = \frac{TP}{TP + FN}, \quad FPR = \frac{FP}{FP + TN} \tag{11}$$

Where TP (true positive) is the number of correct detections of smoke; FN (false negative) is the number of frames which have smoke but not recognized. FP (false positive) is the number of frames which do not have smoke but recognized as smoke; TN (true negative) the correct detection of non-smoke. We also considerate the frame number of every test clip, then the average false positive rate ($AFPR$), average true positive rate ($ATPR$) and average frame number are used to compare our method with others.

The results on the eight clips are shown in Fig. 7 and the specific results of the eight clips are shown in Table. 1. In the Table the results of Toreyin's method, B.C. Ko's method and our method are all listed to make comparison. Because Toreyin's method does not give the specific results, we do the

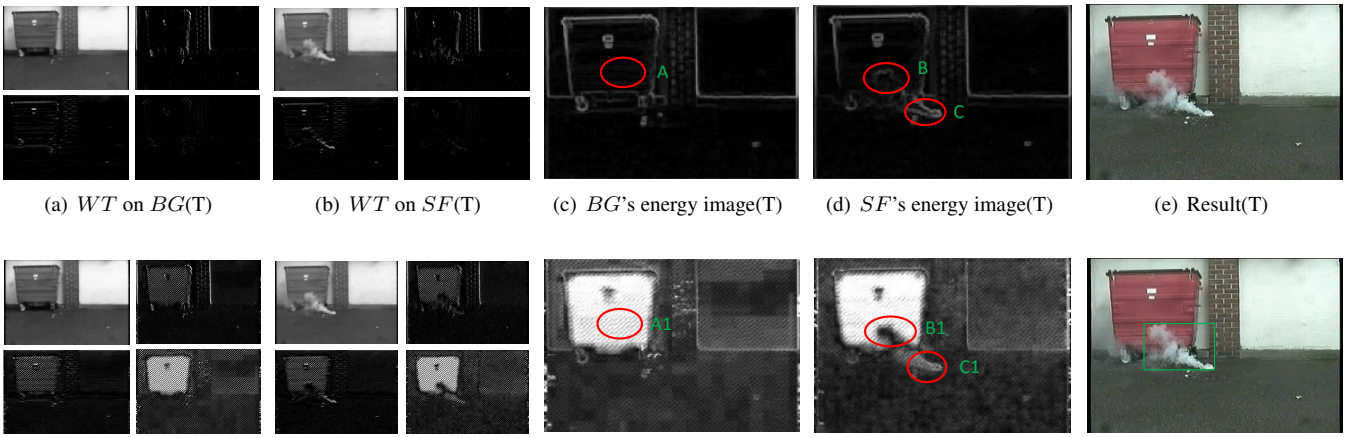

(a) WT on BG(T) (b) WT on SF(T) (c) BG's energy image(T) (d) SF's energy image(T) (e) Result(T)

(f) WT on BG(O) (g) WT on SF(O) (h) BG's energy image(O) (i) SF's energy image(O) (j) Result(O)

Fig. 6. BG and SF are background and smoke frame respectively, WT denotes wavelet transform, T and O denote the methods of Toreyin's and our respectively. T's method used WT directly; however, in our method WT was implemented based on the RGB Contrast-image; the images at the top left corner of (f) and (g) are RGB Contrast-image of BG and SF.

(a) C_1 (b) C_2 (c) C_3 (d) C_4 (e) C_5 (f) C_6 (g) C_7 (h) C_8

Fig. 7. Results of 8 clips.

experiments by ourself based on his paper. In B.C. Ko's paper, he does experiments on five smoke clips and five smoke-like clips, because his $Movie2$ and $Movie5$ are almost the same so we just do experiments on his $Movie5$ which corresponds to our C_7. The rest corresponding relationships are as follows: his $Movie1$ corresponds to our C_5, his $Moive3$ corresponds to our C_2, his $Moive4$ corresponds to our C_6. The '-' in the Table means B.C. Ko does not do experiment on the clip.

Through the specific results showed in the Table. 1, we can see the $ATPR$ of three methods are 77.83, 96.15, 95.9925 and the $AFPR$ of three methods are 0, 1.3, 0.002. The average frame number of our method and Toreyin's method is 928, the average frame number of B.C. Ko's method is 689. Form these results, it can be seen that the proposed method proves more effective than Toreyin's conventional method (We do experiment by ourself based on his paper), especially in $clip_2$ and $clip_5$. The reason may be that in these two scenarios, the background are pure-color and the smoke contains numerous edges which produce rich high frequency energy. Compared with B.C. Ko's method, our method has a better $AFPR$ and a worse $ATPR$. In the C_6 the background is white, it's may lead to the RGB Contrast-image not work well, so the result is not so satisfactory. Although our method has worse $ATPR$ than B.C. Ko's method, we using more simple methods which do not need to train the model and can meet the requirement of real-time.

4. CONCLUSION

Detecting smoke in video surveillance is very important for early fire detection and wavelet based methods are widely used, however, they can't distinguish smoke with general pure color objects and ignore the high frequency produced

Table 1. Compare our method with Toreyin's and B.C. Ko's.

$Clip$		C_1	C_2	C_3	C_4	C_5	C_6	C_7	C_8	$Average$
TPR	Toreyin's	88.2	63.9	84.3	80.34	75.2	78.4	82.5	70.1	77.83
	B.C. Ko's	-	95.5	100	-	-	89.1	100	-	96.15
	Our	89.3	98.75	100	96.34	97.45	87.2	99.4	99.5	95.9925
FPR	Toreyin's	0	0	0	0	0	0	0	0	0
	B.C. Ko's	-	0	0	-	-	0	5.2	-	1.3
	Our	0	0	0.016	0	0	0	0	0	0.002
$Frame$	Toreyin's	800	1600	1200	240	600	890	1100	1000	928
	B.C. Ko's	-	781	475	-	-	980	520		689
	Our	800	1600	1200	240	600	890	1100	1000	928

by smoke. In this paper we introduce the concept of contrast-image and on the basis of contrast-image, background frame's wavelet transformation and current frame's wavelet transformation are obtained respectively. Since edges correspond to high frequency and smoke corresponds to low frequency, we calculate the rate of high frequency and low frequency in order to decide whether the motion area is smoke or not. In addition, color features and optical flow based motion features are also used as clues combined to reach a final decision. Experimental results show our method outperforms the conventional methods remarkably.

5. ACKNOWLEDGMENTS

This work is partially supported by grants from the Chinese National Natural Science Foundation under contract No. 61072095 and No. 61035001.

6. REFERENCES

[1] T.H. Chen, Y.H. Yin, S.F. Huang, and Y.T. Ye, "The smoke detection for early fire alarming system base on video processing," *International Conference on Intelligent Information Hiding and Multimedia Signal Processing*, pp. 427–430, 2006.

[2] F. Yuan, "A fast accumulative motion orientation model based on integral image for video smoke detection," *Pattern Recognition Letters*, vol. 29, pp. 925–932, 2008.

[3] Y. Cui, H. Dong, and E. Zhou, "An early fire detection method based on smoke texture analysis and discrimination," *International Congress on Image and Signal Processing*, vol. 3, pp. 95–99, 2008.

[4] B. Ugur Toreyin, Yigithan Dedeoglu, and A. Enis Cetin, "Wavelet based real-time smoke detection in video," *Signal Processing, Image Communication*, vol. 20, 2005.

[5] B. Ugur Toreyin, Yigithan Dedeoglu, and A. Enis Cetin, "Edge based smoke detection in video using wavelets," *14th European Signal Processing Conf. EUSIPCO*, pp. 1–5, 2006.

[6] Y. Wei, Y. Chunyu, and Z. Yongming, "Based on wavelet transformation fire smoke detection method," *International Congress on Electronic Measurement & Instruments*, pp. 872–875, 2009.

[7] S. Calderara, P. Piccinini, and R. Cucchiara, "Smoke detection in video surveillance: A mog model in the wavelet domain," *International Conference on Computer Vision Systems*, pp. 119–129, 2009.

[8] R.T. Collins, A.J. Lipton, and T. Kanade, "A system for video surveillance and monitoring," *American Nuclear Society 8th Topical Meeting on Robotics and Remote Systems*, pp. 25–29, 1999.

[9] D. Walther and C. Koch, "Modeling attention to salient protoobjects," *Neural Networks*, vol. 19, pp. 1395–1407, 2006.

[10] S.S. Beauchemin and J.L. Barron, "The computation of optical flow," *ACM Computing Surveys*, vol. 27, pp. 433–466, 1995.

[11] B.C. Ko, J.Y. Kwak, and J.Y. Nam, "Wildfire smoke detection using temporospatial features and random forest classifiers," *Optical Engineering*, vol. 51, January 2012.

[12] T. Jakovcevic, L. Seric, and D. Stipanicev, "Wildfire smoke-detection algorithms evaluation," *VI International Conference on Forest Fire Research*, pp. 1–12, 2010.